TRANSIENT EFFECTS IN ISOPHOT DATA: STATUS OF MODELLING AND CORRECTION PROCEDURES[1]

J.A. ACOSTA–PULIDO

Max–Planck–Institut für Astronomie
Königstuhl 17, D–69117 - Heidelberg (Germany)
ISO Science Operations Centre
Astrophysics Division, Space Science Department of ESA
VILSPA - P.O. Box 50727 - Madrid (Spain)
Instituto de Astrofisica de Canarias
E-38200, La Laguna - S/C Tenerife (Spain)

C. GABRIEL

ISO Science Operations Centre
Astrophysics Division, Space Science Department of ESA
VILSPA - P.O. Box 50727 - Madrid (Spain)

AND

H.O. CASTAÑEDA

Max–Planck–Institut für Astronomie
Königstuhl 17, D–69117 - Heidelberg (Germany)
ISO Science Operations Centre
Astrophysics Division, Space Science Department of ESA
VILSPA - P.O. Box 50727 - Madrid (Spain)
Instituto de Astrofisica de Canarias
E-38200, La Laguna - S/C Tenerife (Spain)

Abstract. The calibration of ISOPHOT observations is hampered in many cases by the transient response of the detectors. Here we outline the behaviour observed in flight for the different ISOPHOT detectors. We also present some of the procedures which are currently used to correct transient effects and their implementation in the ISOPHOT Interactive Analysis.

1. Introduction

ISOPHOT is one of the four scientific instruments on board the ISO satellite. It consists of three sub–systems: (i) an aperture photopolarimeter, with three different single pixel detectors (P1, P2 and P3), (ii) a grating spectrophotometer, containing two 64 pixel arrays (SS and SL), and (iii) two far–IR cameras of 9 (C100) and 4 pixels (C200), respectively. P1 and SS/SL use Si:Ga photoconductors as detector elements, P2 uses Si:B, whereas P3 and C100 use unstressed and C200 stressed Ge:Ga detectors, respectively. A more detailed description of ISOPHOT observing capabilities and performance can be found in Lemke *et al.* (1993 and 1996).

One challenge in the calibration of the ISOPHOT instrument is the transients in the signals of the detectors. Transient effects are a typical behaviour of extrinsic photoconductors, as used in ISOPHOT, if they are operated at low temperatures and are exposed to low background illumination. A generally observed effect is a slow response after a change in the illumination. One of the main reasons for this behaviour is the use of implanted contacts, needed to achieve ohmic contact between the metallic wire and the photoconductor (see for example Haegel, Latasa and White, 1993).

In this paper we will present the procedures which are currently used to correct transient effects in the ISOPHOT measurements. Three different possibilities are offered within the ISO**P**HOT **I**nteractive **A**nalysis (**PIA**[2]):

- Drift recognition: the stabilized part of the measurement is identified, starting from the last measured signal.
- A physical model developed by Fouks and Schubert applied to SS/SL.
- An empirical solution for FIR detectors (Ge:Ga), based on exponential functions.

Superimposed on the signal transients there is a long term drift effect that needs to be quantified by the calibration: the responsivity of the detectors systematically changes with time due to hits by high energy particles. This will be addressed in some more detail in sect. 6.

2. Drift recognition

The first indication of transient effects is any increase or decrease of the signal observed in some measurements. However, transient effects can have

[1]Based on observations with ISO, an ESA project with intruments funded by ESA Member States (especially the PI countries: France, Germany, the Netherlands and the United Kingdom) and with the participation of ISAS and NASA.

[2]PIA is a joint development by the ESA Astrophysics Division and the ISOPHOT Consortium. For more detailed description see Gabriel *et al.* 1997

such long time scales that no apparent trend is seen during the observation. An automatic procedure to recognize the stable part in the data was introduced in PIA. It is based on a trend analysis of the signal values. It discards signals from the beginning of the measurement until a stable region is found, or, alternatively, a minimum number of data points are left (typically 7 signals or the last 8 s). The algorithm is based on the sign test. The result of this analysis is an assessment whether a measurement is stable, partially stable or unstable. Depending on the result a certain part of the data is selected to derive the final value. Currently, this procedure is used in the derivation of signals in the automatic Offline Processing.

3. Fouks–Schubert model applied to ISOPHOT-S

3.1. PRE–FLIGHT WORK

Schubert *et al.* (1995) have shown, using data obtained during the ISOPHOT pre–flight calibration, that the non–linear transient response of the detector array SS/SL can be described by a simple analytical function. This function was derived based on a physical model developed by Fouks and Schubert (1995) and references therein. The time dependence of the signal $S(t)$ is described by:

$$S(t) = \beta S_\infty + \frac{(1-\beta)(S_{ini} - \beta S_\infty)S_\infty}{S_{ini} - \beta S_\infty + (S_\infty - S_{ini})\ exp(-(t-t_{ini})/\tau_j)}; \quad \tau_j = \frac{E}{\beta S_\infty}$$

β represents the fraction of the stable signal which is reached almost inmediately after a flux change. E determines the timescale of the transient response. S_{ini} and S_∞ represent the initial and final values of the photocurrent, respectively. E and β are parameters which are specific for each pixel/detector.

Another important theoretical result is the prediction of the change in photocurrent after a certain flux change, by the following expression:

$$S^n_{initial} - S^{n-1}_{final} = \beta(S^n_\infty - S^{n-1}_\infty),$$

where $S^n_{initial}$ and S^{n-1}_{final} are the values of the photocurrent before and after the n-th flux step, respectively. The above expression will be refered hereafter as the "signal jump condition".

The parameters E and β were determined during the pre–flight calibration. Very long stabilization times were found for low fluxes (for example $\sim$ 20 min at a flux of 1 Jy). Typical values for β and E are 0.6 and 2.5, respectively. The first 15 pixels in the SS (2.5–3 μm) array showed very slow responses compared to the rest.

3.2. IN–ORBIT EXPERIENCE

The staring observations cannot be well reproduced using the expression above, which is a monotonic function. We found very often peculiar drift curves with a characteristic hook shape, especially at short wavelength pixels. The differences found with respect to the ground calibration can be likely attributed to the different operational conditions: detectors are switched–on prior to any observation and switched-off afterwards, opposite to the more continuous ground calibration; high energy radiation particle hits may also affect the transient behaviour.

Therefore, for staring modes, a different approach was undertaken in order to be able to calibrate the data without having to do a prediction of the stabilized photocurrent. A direct comparison is made of the temporal evolution of the photocurrent between measurements of a target and a calibration star of similar flux. This method, called the "dynamical calibration", relies on the hypothesis that the transient response is very reproducible under similar illumination conditions and history. This is the case for SS/SL as the AStronomical Observation Template always has a fixed sequence starting with a dark current check of 32 s followed by the sky measurement. The observing mode of SS/SL is very simple and always contains a short dark current check before the on-target measurement.

On the other hand chopped measurements for which the flux history is well known, can be well modelled using a combination of both the signal jump condition and the temporal behaviour for a fixed flux level (see Fig. 1). The preflight values of the parameters β and E were checked using special observations, finding a very good agreement. The implementation of this correction is available in PIA versions later than 6.4. A more detailed description will be given elsewhere (Acosta–Pulido et al, in preparation).

In principle, detectors P1 and P2 could be treated in a similar way as SS/SL, since they are manufactured of similar material, however detailed studies have to be undertaken to verify this.

4. Empirical solution for ISOPHOT-FIR detectors

The basic transient behaviour of detectors P3, C100 and C200 (all based on Ge:Ga) after a flux change can be described as follows:

1 - There is an initial jump of constant relative height w.r.t the final signal difference. This has been observed in chopped measurements where the flux modulation is fast. There is theoretical support for this feature coming from numerical computations (Fig. 5 in Haegel *et al.* , 1996).
2 - A short term ($\leq$ 10 s) response follows, which shows a characteristic form known as "hook response" (see Figs. 2 and 3). This part looks

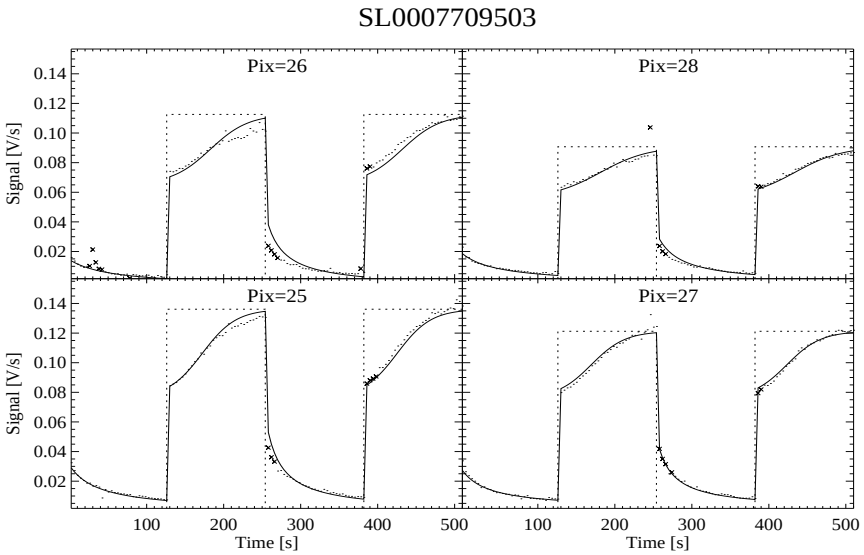

Figure 1. Example of a chopped measurement (alternating between off and on–source observation) for several pixels of detector SS. The Fouks–Schubert model fitted to the data (dotted line) is represented by the solid line. The dashed boxes represent the predicted final signal.

different for the individual detectors: for P3 and C100 it appears like overshooting in case of flux increase and undershooting in case of flux decreases, whereas for C200 it is in general a very fast overshooting.

3 - A long term response follows, which can be well modelled by an exponential function in most cases (see Figs. 2–5).

4 - The long term response exhibits a time constant which decreases for high fluxes, whereas it increases dramatically for low fluxes.

We present here a solution based on a single exponential function, which can be written as the following expression:

$$S(t) = S_\infty + (S_{ini} - S_\infty)\ exp(-t/\tau); \quad \tau = \frac{E}{S_\infty^\alpha}.$$

The first analysis shows that τ is inversely proportional to the final signal, $S\infty$, in log–log scale (see Fig. 6). Therefore τ can be written as an inverse power law function of $S\infty$. The parameter α describes the behaviour of the transient effects with the illumination and E is a normalization constant. E and α are parameters which have to be determined for each detector/pixel. In the case of the Fouks–Schubert function α is equal to unity. If the proposed function is a good description of the transient behaviour of the considered detectors, those parameters can be fixed. The

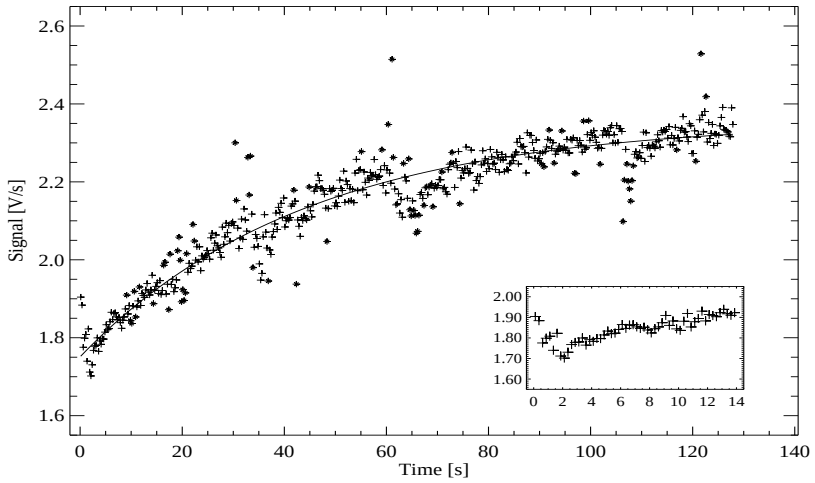

Figure 2. Typical transient behaviour of detector P3 at intermediate flux level ($\sim$ 11 Jy at 100μm). The measured signals are represented by plus sign symbols. Detected glitches are marked by crosses. The exponential model is represented by the continuous line through the data points. The initial signal sequence is shown in the inset, where the hook response is clearly recognized.

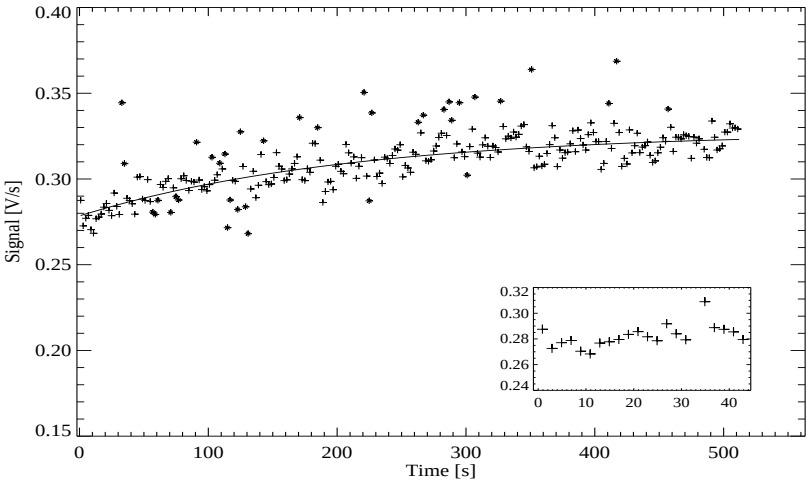

Figure 3. Typical transient behaviour of detector P3 at low flux level ($\sim$ 2 Jy at 100μm). The meaning of the symbols is as in Fig. 2.

stabilized signal is obtained by fitting the above function to the measured signals and leaving S_{ini} and S_{∞} as free fit parameters.

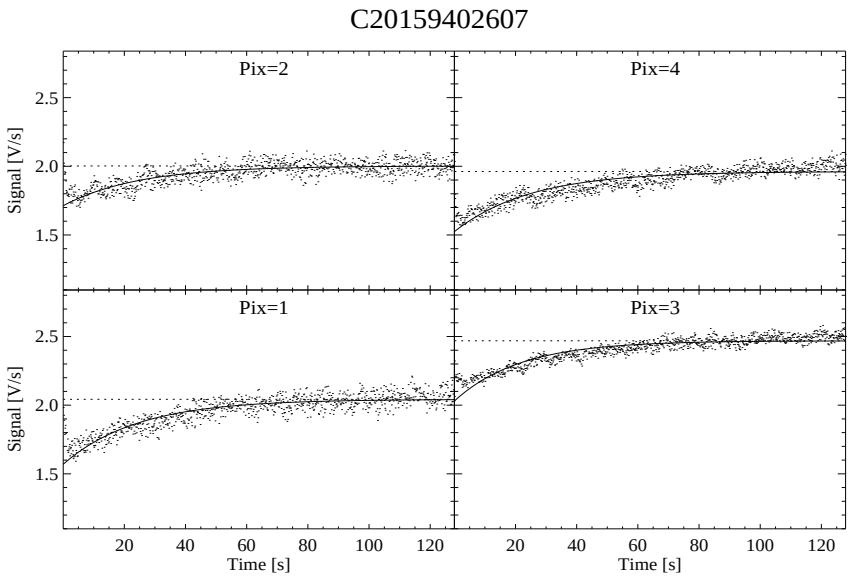

Figure 4. Typical transient behaviour of the four C200 pixels at high flux level ($\sim$ 60 Jy at 150μm). The dots represent the measured signals, the solid line the fit and the dashed horizontal line the predicted final signal level.

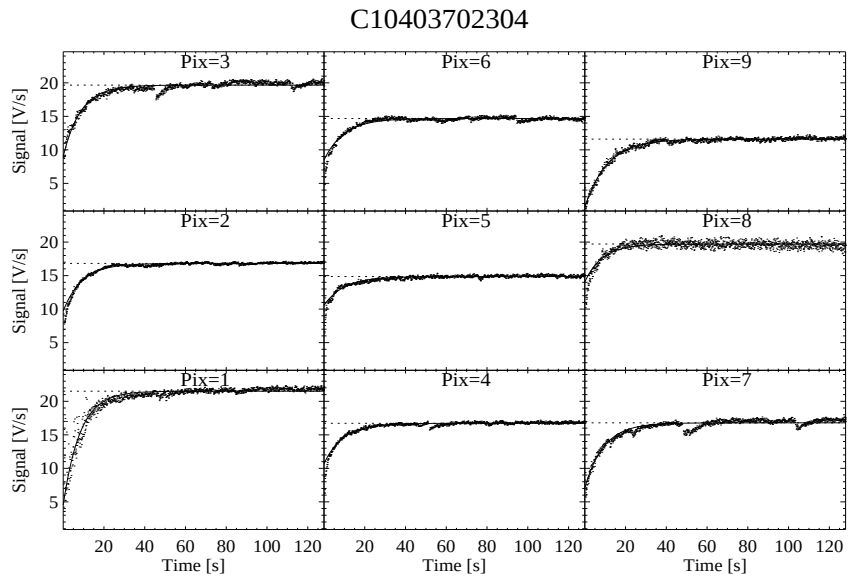

Figure 5. Typical transient behaviour of detector the nine C100 pixels at high flux level ($\sim$ 75 Jy at 80μm). The meaning of the symbols is as in Fig. 4.

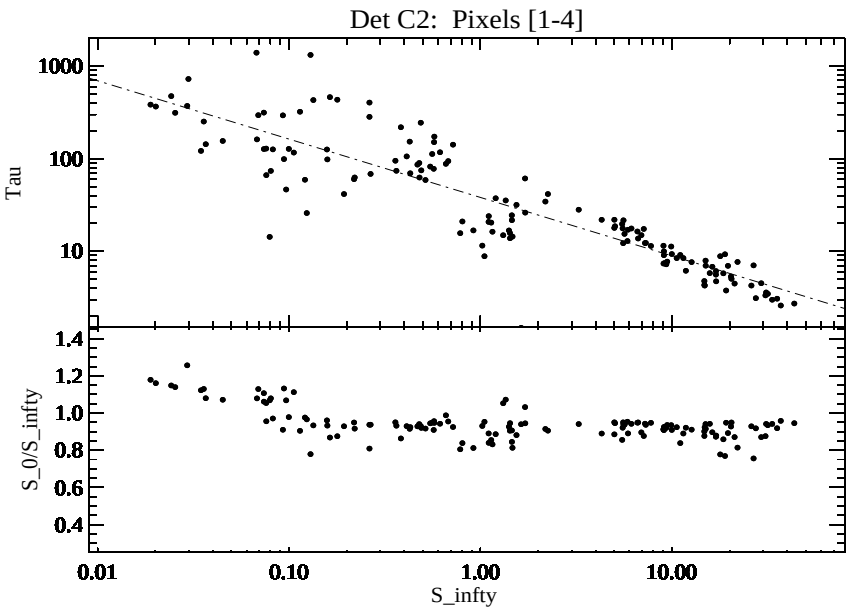

Figure 6. Time constant determination for detector C200 (including all pixels). The ratio of initial to final signal obtained from the model fit is presented in the bottom panel.

4.1. DETERMINATION OF TIME CONSTANTS

We have determined the parameters E and α for the detectors P3, C100 and C200, using a large set of long measurements. The measurements were selected if a clear transient behaviour was present, and they are long enough that at the end the photocurrent is close to stabilization. Nevertheless, our data set may suffer some selection bias: transient behaviour with very long time constants (> 1000 s) will not be detected because of the limited observing time; the flux history may influence the transient as well as the switch–on of the detector every time an observation starts. In the process of determining E and α we fitted each measurement by leaving all parameters free in the above expression and rejecting those fits where the residual RMS per degree of freedom was larger than 3.

We present in Fig. 6 an example of the best fitting parameters. Clear correlations between τ and S_∞ can be established. From a least square fit we have determined the values of E and α and the results are presented in Table 1, together with the correlation coefficient r. It was found that for P3 and C200 the correlation is very good and is worse for C100.

We perfomed tests using an independent set of measurements other than those used for determining the time constants. The resulting χ^2 distribu-

TABLE 1. Time constants for the empirical model.

Detector	E	α	r	β
P3	87 ± 8	0.79 ± 0.05	-0.79	~ 0.34
C100	36 ± 3	0.48 ± 0.04	-0.63	~ 0.30
C200	38 ± 2	0.63 ± 0.03	-0.89	~ 0.85

tions are very narrow and peak around 1. The worst case is the detector C100, for which the χ^2 distribution for all pixels (except pixel 8) is wide and values around 2-3 are frequent. The low frequency noise which affects detectors C100 and P3 when measuring faint targets is likely limiting the goodness of the fit.

We present in Fig. 7 an example of the application of the model for a measurement with detector C100: using the full measurement time of 512 s an error of 6% between the direct measurement of the signal and the model prediction is found. A comparison of the estimates of the final signal using only the first 32 s gives the following results: the value obtained from the drift recognition (Section 2) is too low by 30%, whereas the value obtained from the empirical model is lower by only 12%. This example demonstrates that the use of the drift modelling significantly improves the photometric accuracy of relatively short measurements.

We estimated the fraction of the final signal which is affected by the slow transient component, *i.e.* the signal difference between the value reached at the initial jump and the final value. The magnitude of this component combined with the time constant determines the accuracy of any measurement after a certain time. For example, a long time constant is not so relevant, if the fraction of the slow component is small compared to the total signal. The magnitude of the slow component can be estimated from the initial jump after a flux change and the knowledge of the final stable current (see "signal jump condition" in Section 3). This has to be derived from chopped measurements where the flux changes are like a step–function. Raster observations cannot be used, because the flux varies gradually as the telescope slews to a different sky position. Results for detectors P3, C100 and C200 are presented in Table 1, β represents the fraction of the total signal difference which is achieved immediately after the flux change. It has been found theoretically that the magnitude of the slow component increases with the photoconductive gain, G (Haegel *et al.* 1996). G depends on the material, the electric field and the dimensions of the detector. Detectors P3 and C100 are manufactured of the same material but they have different bias voltages and dimensions, yielding $G[C100] > G[P3]$, which is consistent with a

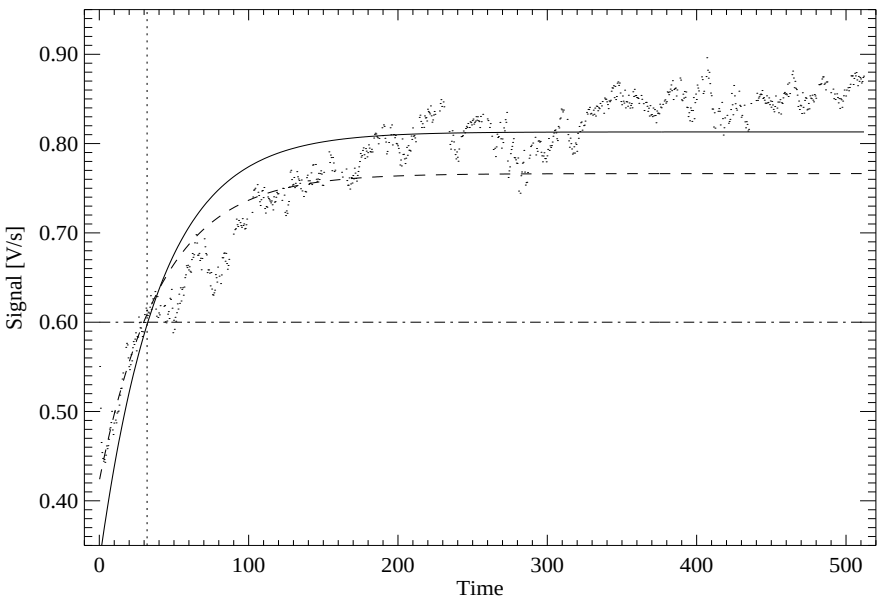

Figure 7. Measurement of a intermediate brightness ($\sim$ 8 Jy at 100μm) source using detector C100 (central pixel). The measured signals are shown by dots. The solid line represents the empirical model described in the text using data up to 512 s. The final signal was also predicted using only the first 32 s (marked by the vertical dotted line) in two ways: by the drift recognition method (Section 2), shown as the dashed–dotted line and by the exponential model (Section 4), shown as the dashed line.

larger fraction of the slow component for C100.

5. Implementation in PIA

Following the description of the correction methods above, the approach is to fit the observed signals and to predict the final stabilized value. The fitting procedure begins with the estimate of suitable starting parameters corresponding to the current data and the model to be used. The minimization of χ^2 is done in two steps: a first parameter determination is done using a downhill simplex method (AMOEBA), and these parameters are used as starting values for a second fit using a gradient expansion algorithm.

We have developed a graphical user interface (see Fig. 8) which includes the possibility of: (a) choosing among different functions with their corresponding parameter initialization depending on the detector, (b) fixing or releasing parameters in the fit, setting specific values or limits and (c) setting selection criteria, tolerance degree of the fit and weighting method to be applied. All the start parameters can be tested and fine tuned before all

detector pixels are processed. After the bulk processing, PIA also provides the possibility to examine interactively the fit results and re–evaluate non–satisfactory fits. A flag system has been developed which checks whether a number of criteria (*e.g.* convergence of the minimization, χ^2 is below a certain threshold, free parameters within range) are fulfilled. This makes the analysis of large data sets very efficient, while permitting fast and deep data correction.

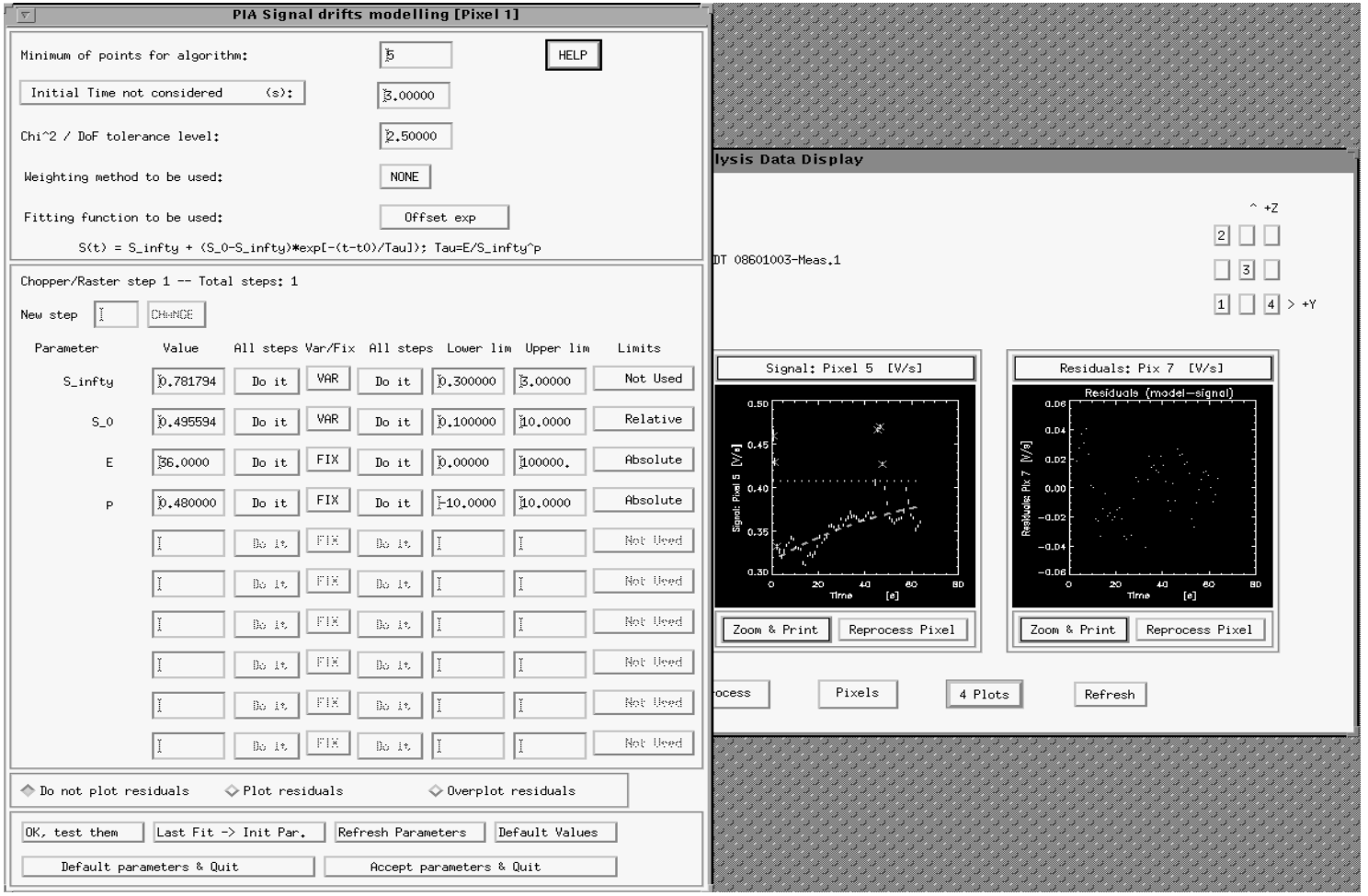

Figure 8. PIA Graphical user interface for treatment of transient correction: The left side shows the interface which allows to test several drift models, change the parameters, etc. The right side displays a higher level interface which allows to inspect the results of drift modelling for all pixels at the same time, w.r.t. see the expected final value, the residuals of the fit, etc. For a detailed description of its use please refer to the PIA Users Manual (http://isowww.estec.esa.nl/manuals/PHT/pia/um/pia_um.html).

TABLE 2. Mean responsivity variation along an ISO revolution.

Detector	No Recuring $(R_e - R_i)/R_i$	Recuring $(R_m - R_i)/R_i$	Recuring $(R_e - R_m)/R_m$
P1	≤ 0.05	...	...
P2	~ 0.3	...	...
P3	~ 1.86	0.5	0.5
C100	1.9	0.33	0.75
C200	0.2	0.1	0.1

6. Variation of detector responsivity along a revolution

In addition to the the signal transients due to illumination changes, there is a long term drift effect, which appears even under constant illumination and with the detector signal adjusted to that level. There are responsivity variations caused by high energy particle hits (see Lemke *et al.* 1993, and very recently Patrashin in these proceedings). On the high parts of the ISO orbit these are mainly cosmic ray glitches, whereas closer to the radiation belts stronger variations due to the space weather conditions (see contribution by H. Castañeda in these proceedings) can occur. In order to restore the nominal responsivity, all detectors were cured after passing the radiation belts, at the beginning of each ISO science revolution. An additional re–curing was introduced at the middle of the revolution for the FIR Ge based detectors. Nevertheless, each ISOPHOT science observation contains at least one measurement with the internal calibrator, which can be used as a reference to determine the actual value of the responsivity.

The responsivity generally varies within long timescales as compared to common observing times, as it will be shown below. We performed a statistical study of its variation along an ISO revolution using a large set of observations, in which the values of actual responsivities were derived by the automatic Off–Line Processing Pipeline (OLP). The responsivity variation along the orbit position for each detector/pixel was fitted by a smooth curve (linear or parabolic fit at maximum). These curves are used to correct the default responsivity which is used in PIA and OLP. The mean variation of the responsivity for each detector is presented in Table 2, where R_i, R_m and R_e represent the responsivity at the beginning, the middle and the end of the science window of the ISO revolution.

We also investigated the temporal variation of the responsivity on shorter timescales using raster observations which contain two measurements of the internal calibrator, at the beginning and at the end. We found that responsivity changes depend on the in–band power received by the detector (see

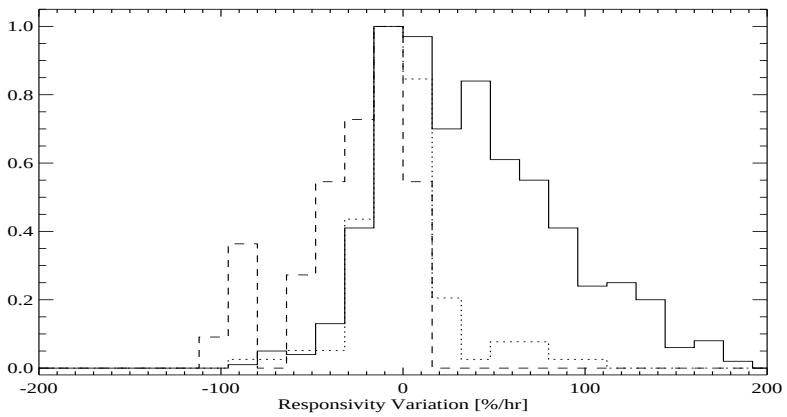

Figure 9. Histogram showing the temporal variation of the responsivity for the central pixel of detector C100 and three different in–band power ranges. The continuous line represents the variation for low inband-power ranges, the dotted line for intermediate ranges and dashed line for high ranges.

Fig. 9): For high powers the responsivity stays roughly constant, it can even decrease, like a recuring effect. For low powers the responsivity increases drastically, with a mean rate of $\sim 40\%\ hr^{-1}$ for C100, $\sim 25\%\ hr^{-1}$ for P3 and moderately with a mean rate of $\sim 2\%\ hr^{-1}$ for C200. The rates for P3 and C100 are large compared to what is statistically observed along a revolution (see Table 2). There are several reasons which may explain such a discrepancy, among others we remark: the responsivity varies differently depending on the incoming infrared flux. On the other hand it is not yet clear whether the responsivity variation is different for detector measurement or stand–by mode.

7. Concluding remarks and future work

The application of the Fouks–Schubert physical model to the detector SS/SL is limited to chopped observations. A completely different approach called "dynamical calibration" is being explored for staring observations with good success.

An empirical correction based on an exponential function is offered for FIR ISOPHOT detectors. It has been demonstrated to be a successful solution for modelling the slow transient component in a large number of measurements. Tests have shown that the use of drift modelling upon the first 16 s or 32 s significantly improves the estimate of the final signal. This is especially relevant to the relatively short measurements of the internal calibrator for a given science observation, which are used as references in the

photometric calibration. Nevertheless, a detailed analysis of the transient curve, especially for C100, reveals the presence of more than one time constant. We have also explored a solution consisting of a linear combination of two exponential functions with satisfactory results. The main difficulty is to determine the relative importance of the two components. We will continue to explore this solution. A linear combination of three exponential functions has been proposed already by other authors (Church *et al.* 1996; Fujiwara *et al.* 1995).

We have not paid much attention to the initial seconds after a flux change, where the hook response is observed. We have not considered it here, since it is not relevant for the in general long observation times. However, it may be important when treating high frequency chopped measurements. Sclar (1984) has proposed a description of the transient behaviour which reproduces the hook shape and may be applicable to our detectors.

The approach described in this paper is basically intended for applications with one flux step, but afterwards constant flux. We have started to explore a solution combining the exponential function and the signal jump condition, which is applicable to raster measurements where the flux changes for different sky positions. A more detailed discussion can be found in Acosta–Pulido (1998).

The responsivity variation along an ISO revolution affects principally the detectors P3 and C100. Furthermore, the responsivity increase is larger when the received flux is lower, whereas at high fluxes it shows a very stable behaviour.

8. Acknowledgments

We are indebted to Dr. Ulrich Klaas for a very careful reading of this paper and his valuable support. It is a pleasure to acknowledge to Dr. Nancy Haegel and Dr. Joseph Schubert for their valuable advise during the period of this investigation. ISOPHOT was funded by the Deutsche Agentur für Raumfahrangelegenhoiten DARA, the Max–Planck Society, the Danish, British and Spanish Space Agencies and several European and American Institutes.

References

Acosta–Pulido, J.A. (1998) *Comparison of ISOPHOT and ISOCAM/IAS transient correction* in **http://www.iso.vilspa.esa.es/users/expl_lib/PHT_list.html**

Church, S.E., Price, M.C., Haegel N.M., Griffin M.J. and Ade, P.A.R. (1996) *Applied Optics* **Vol. 35 no. 10**, pp. 1597

Fouks, B.I. and Schubert, J. (1995) *Proc SPIE* **Vol. 2475**, pp. 487

Fujiwara, M., Hiromoto, N. and Araki K. (1995) *Proc. SPIE* **Vol. 2552**, pp. 421

Gabriel, C., Acosta–Pulido, J.A., Heinrichsen, I., Skaley, D., Morris, H. and Tai, W-M. (1997) *Proc of ADASS VI Conf.*, eds. G. Hunt, and H.E. Payne, pp. 108
Haegel, N.M., Latasa, C.A. and White, A.M. (1993) *Appl. Phys. A* **Vol. 56**, pp. 15
Haegel N.M., Newton, C., Simoes, J.C. and White, A.M. (1996) *30th ESLAB Symp.*, pp. 15
Lemke. D., Klaas, U., Abolins, J. *et al.* (1996) *A. & A.* **Vol. 315**, pp. L64
Lemke. D., Wolf, J., Schubert, J. and Patrashin, M. (1993) *Proc SPIE* **Vol. 1946**, pp. 261
Sclar, N. (1984) *Prog Quant. Electr.* **Vol. 9**, pp. 149
Schubert, J., Fouks, B.I., Lemke. D. and Wolf, J. (1995) *Proc SPIE* **Vol. 2553**, pp. 461